# Electronic Supplementary Information

## Electrochemically Controlled ON/OFF Switching of $NaBH_4$ Hydrolysis Based on NiMoN@NC for On-Demand Hydrogen Production

Baoying He, [a] Shuxian Zhuang, [b] Xuefeng Tai, [a] Ao Xie, [b] Weihao Lou, [a] Yang Tang, [a,*] Yongmei Chen, [b] Pingyu Wan[b]

[a]Institute of Applied Electrochemistry, Beijing University of Chemical Technology, Beijing 100029, China.
[b]National Fundamental Research Laboratory of New Hazardous Chemicals Assessment & Accident Analysis, Beijing University of Chemical Technology, Beijing 100029, China.

Corresponding Author
*Yang Tang
Email: tangyang@mail.buct.edu.cn

## MATERIALS AND METHODS

### Materials and chemicals

All the chemicals were used as received without further purification. Nickel chloride hexahydrate (98%), ammonium molybdate tetrahydrate (99.9%) and sodium borohydride (98%) were purchased from Shanghai Aladdin Biochemical Technology Co., Ltd. Sodium hydroxide (96%), ethanol absolute (99.7%) and dicyandiamide (DCDA) were obtained from Tianjin Fuchen Chemical Reagents Factory. N, N-Dimethylformamide (DMF), hydrochloric acid (36~38%) and acetone (99.5%) were customized from Tianjin Damao Chemical Reagents Factory. Nafion (5 wt.%) were customized from Zebrest Technology Co., Ltd.

Ni foam was purchased from Shanxi lizhiyuan battery material Co., Ltd. Commercial Pt/C (20 wt.%) was bought from Shanghai Hesen Electric Co., Ltd. Graphite rod electrode and Pt foil electrode were customized from Tianjin Aida Hengsheng Technology Development Co., Ltd.

### Synthesis of NiMoN@NC catalyst

The Ni foam (3.8 × 4 $cm^2$) was sonicated with acetone, hydrochloric acid, ultrapure water and ethanol in turn, and the cleaned Ni foam was dried in the air.

In a typical synthesis process, $NiCl_2 \cdot 6H_2O$ (0.99 g) and $(NH_4)_6Mo_7O_{24} \cdot 4H_2O$ (1.29 g) were dissolved in 70 ml ultrapure water under stirring for 1 h. The as-prepared Ni foam was immersed into the above solution, and transferred into a 100 ml Teflon-lined stainless-steel autoclave. The autoclave was sealed and heated at 150 ℃ for 6 h in a blast oven. After the autoclave cooled down to ambient temperature, the yellow $NiMoO_4$/Ni foam was taken out and rinsed with large amount of ultrapure water, then dried in a vacuum drying oven at 70 ℃ for 24 hours.

To synthesize the NiMoN@NC catalyst, a $NiMoO_4$/Ni foam was placed on the downstream side of a furnace, and 2 g DCDA was placed in another porcelain boat on the upstream side. Subsequently, the temperature was increased at 3 ℃ $min^{-1}$ and kept at 500 ℃ for 1 h to ensure full preheating of DCDA, and then increased to 600 ℃ and kept for 2 h in Ar atmosphere. The black NiMoN@NC catalyst was obtained after cooling to room temperature. By increasing the amount of DCDA can obtain the NiMoN@NC-3 g catalyst with thick carbon layer.

### Synthesis of NiMo and NiMoN catalysts

The above $NiMoO_4$/Ni foam was placed on a porcelain boat, which was located in the middle of the furnace. Subsequently, temperature was increased at 3 ℃ $min^{-1}$ to 600 ℃ and kept for 2 h in $H_2$ : Ar=1:4 ($NH_3$ : Ar=1:4) atmosphere. The black NiMo (NiMoN) catalyst was obtained after cooling to room temperature.

### Preparation of commercial Pt/C electrode

A Ni foam (1 × 1 $cm^2$) was cleaned in the same operation as synthesis of $NiMoO_4$/Ni foam. 720 μL DMF and 80 μL Nafion (5 wt.%) was mixed, and 5.00 mg commercial Pt/C (20 wt.%) powder was dispersed in the above solution and sonicated

for 30 min to obtain ink. Then 160 μL of the ink was dripped on the Ni foam and dried in an infrared oven. The area mass loading of Pt/C is about 1 mg $cm^{-2}$.

**Characterization**

The surface morphology of catalysts was observed by a Zeiss Supra 55 field emission scanning electron microscope at an accelerating voltage of 10 kV. The crystallographic structure of catalysts was measured by a RigakuD/MAX 2500VB2+/PCX diffractometer with Cu Kα radiation (hυ = 8047.8 eV). To analyze the electronic states of the catalyst, X-ray photoelectron spectroscopy (XPS) measurements were performed on an ESCALAB 250, of which the X-ray source was Al Kalph 150 W. High-resolution transmission electron microscopy (HRTEM) examination was carried out on a JEOL JEM-2100.

**Electrochemical measurements**

The electrochemical measurement of the prepared electrodes was carried out on a electrochemical workstation (CHI 760E, Shanghai, China) in a typical three-electrode system, in which the carbon rod and the standard calomel electrode (SCE) were used as counter electrode and reference electrode respectively. The Cyclic voltammetry (CV) of Commercial Pt-based electrodes, NiMo, NiMoN and NiMoN@NC electrodes were performed in different potential ranges at a scan rate of 5 mV $s^{-1}$ in 1 M NaOH with and without 0.05 M $NaBH_4$. The ON/OFF chronoamperometry tests were carried out at two different potentials for 600 s under stirring of the solution, of which the ON potential was set around the open circuit potential and the OFF potential was set at the midpoint value of the overlapping interval of the CV curves.

All the potentials mentioned in this work were calibrated to the reversible hydrogen electrode (RHE) scale.

$$E\ vs.\ RHE = E\ vs.\ SCE + 0.2415\ V + 0.059 \times pH = E\ vs.\ SCE + 1.078\ V$$

The calibration was performed in hydrogen-saturated 1 M NaOH with 0.05 M $NaBH_4$, using a platinum wire electrode as working electrode. As shown in Fig. S13 (ESI†), CV curves were measured near the open circuit potential with a scan rate of 1 mV $s^{-1}$. The calibrated potential (-1.078 V) at 0 mA $cm^{-2}$ was used to correct the potential of saturated calomel to reversible hydrogen.

**The hydrogen collection method**

The volume of hydrogen was equivalent to the volume of displaced water by using the water displacement method. The hydrogen production equipment was an airtight container, in which 100 ml solution containing 1 M NaOH and 0.05 M $NaBH_4$ was injected. A water bath was used to control the test temperature. The produced hydrogen entered a conical flask through a pipeline, and the water inside was squeezed into a liquid collecting device which is sealed with parafilm to protect from evaporation of water. The volume of the drained water was measured by an electronic balance (the accuracy is 0.01 g) connected to a computer automatically.

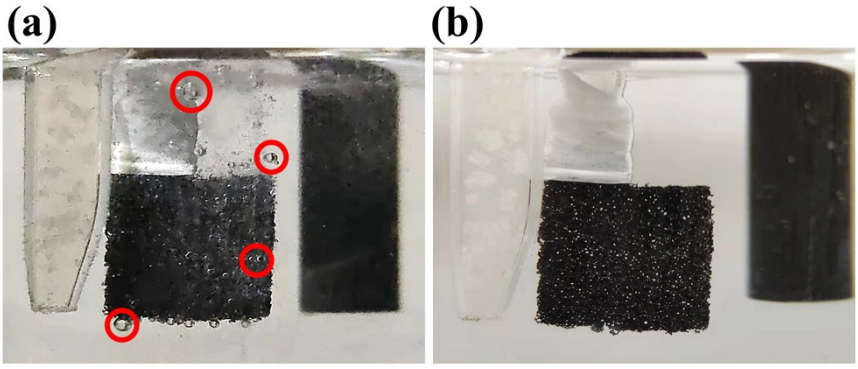


**Fig. S1** The photos of the chronoamperometry test device in (a) ON state and (b) OFF state.

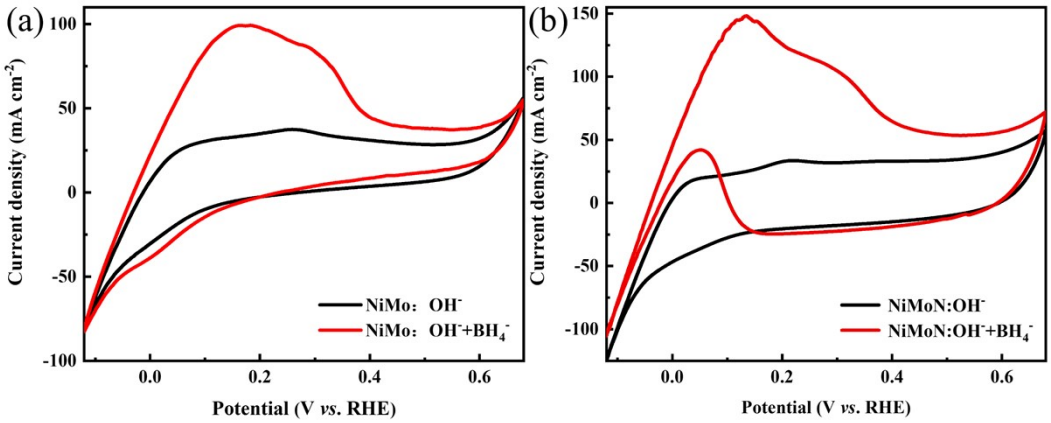


**Fig. S2** CV curves of (a) NiMo and (b) NiMoN in 1 M NaOH with and without 0.05 M $NaBH_4$ at a scan rate of 5 mV $s^{-1}$.

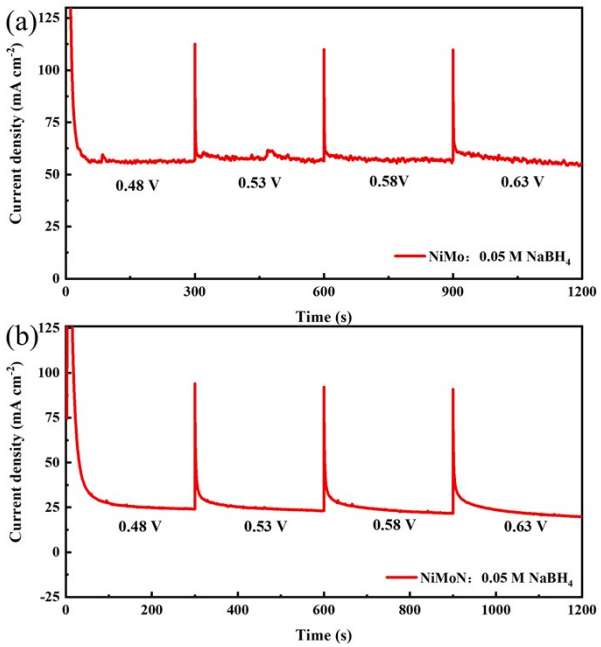


**Fig. S3** The chronoamperometry test of (a) NiMo and (b) NiMoN at different potentials for 300 s in 1 M NaOH with 0.05 M $NaBH_4$.

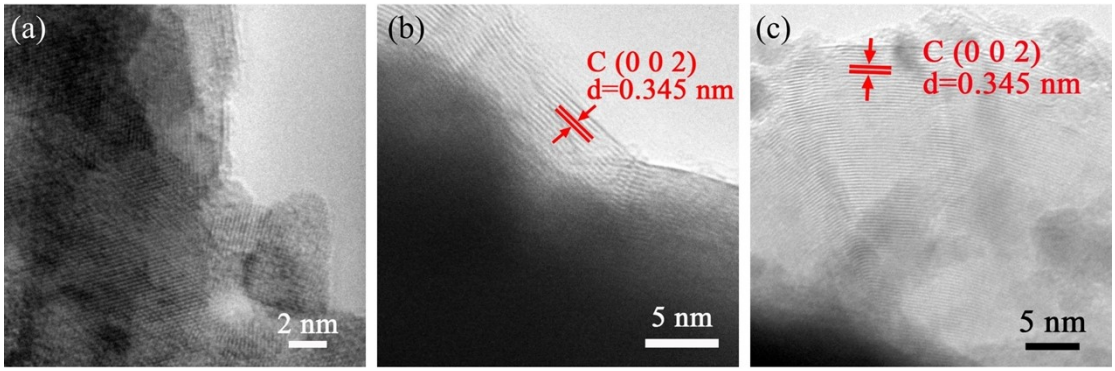


**Fig. S4** The HRTEM images of (a) NiMoN (0 g), (b)NiMoN@NC (2 g) and (c) NiMoN@NC-3 g catalyst.

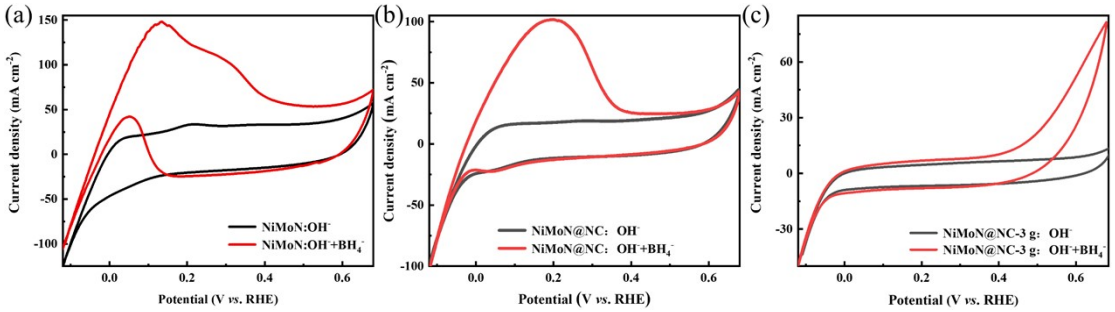


**Fig. S5** CV curves of (a) NiMoN (0 g), (b) NiMoN@NC (2 g) and (c) NiMoN@NC-3 g in 1 M NaOH with and without 0.05 M $NaBH_4$ at a scan rate of 5 mV $s^{-1}$.

By increasing the amount of Dicyandiamide, we obtain NiMoN@NC-3 g catalyst. According to the HRTEM images (Fig. S4), no carbon layer can be notice in NiMoN (0 g) micropillars. There is a carbon layer coated on the surface of NiMoN@NC (2 g) and NiMoN@NC-3 g micropillars, and the lattice fringes measured in Fig. S4b and S4c are both 0.345 nm belonging to (0 0 2) plane of graphite carbon. The carbon layer thickness of optimal NiMoN@NC (2 g) is around 5 nm, and that of NiMoN@NC-3 g is nearly 20 nm which is much thicker than that of NiMoN@NC (2 g).

As shown in Fig. S5a, NiMoN (0 g) exhibits significantly higher anodic current in the presence of $BH_4^-$ than the background current and keep a few bubbles spilling out at the oxidation potential, indicating that the catalyst without carbon layer is too difficult to fully separate the catalyst from the sodium borohydride. On the other hand, the thick carbon layer will obviously impede both the $BH_4^-$ hydrolysis and BOR on the catalyst, owing to obstruction of the $BH_4^-$ adsorption. There is almost no $H_2$ gas releasing from the surface of NiMoN@NC-3 g at the potential from -0.05 to 0.4 V (Fig. S5c), which making that it is hard to observe the phenomenon of ON/OFF switching. That is, the catalyst without carbon layer is unable to leave the catalyst in a completely OFF state, and the thicker carbon layer is harmful to the $BH_4^-$ hydrolysis. In conclusion, the suitable thickness of carbon layer is a key factor for the electrochemically controlled $BH_4^-$ hydrolysis.

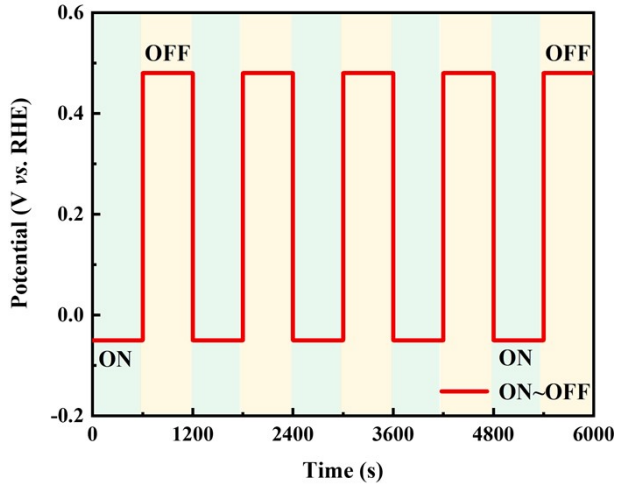


**Fig. S6** The ON/OFF chronoamperometry test of NiMoN@NC in 1 M NaOH with 0.05 M $NaBH_4$ at ON potential (-0.05 V) and OFF potential (0.48 V) for five cycles.

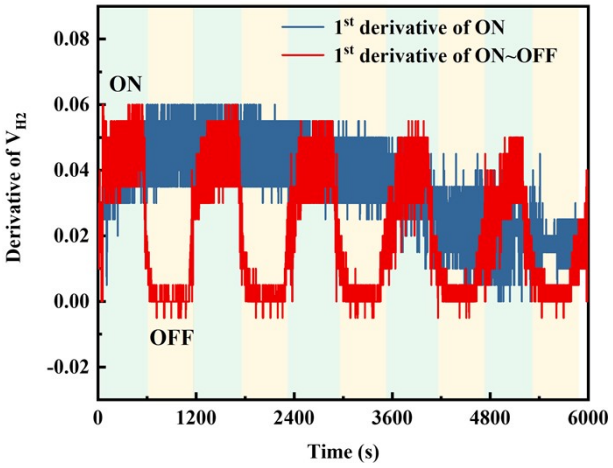


**Fig. S7** The differential analysis of hydrogen volume with respect to time in the ON/OFF switching curve and the continuous ON curve.

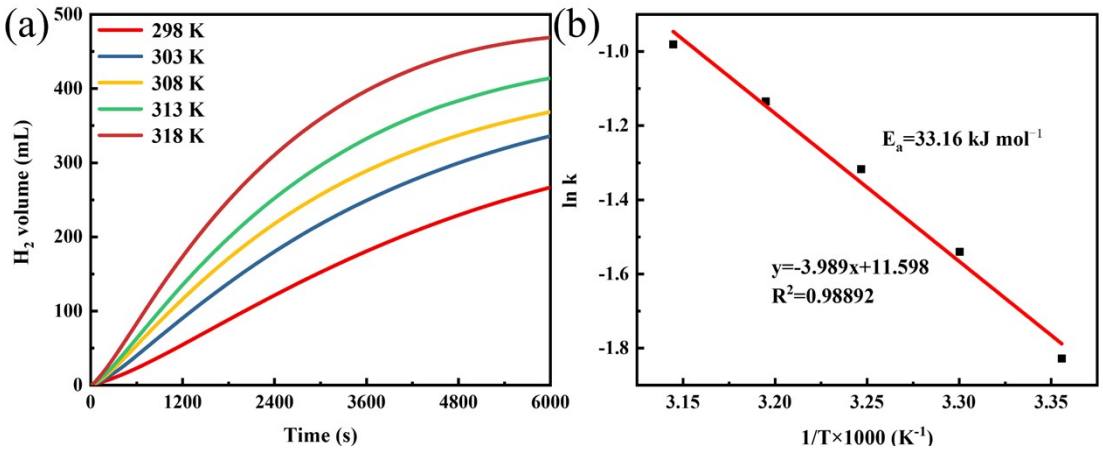


**Fig. S8** (a) The curves of hydrogen volume vs time derived from the ON state of NiMoN@NC in 1 M NaOH with 0.05 M $NaBH_4$ at different temperatures. (b) The linear fitting curve of ln k-1/T.

The Arrhenius equation[1] is as follow.

$$\ln k = \ln A - (\frac{Ea}{RT})$$

k is the HGR constant, A is the pre-exponential factor, $E_a$ is activation energy, R is gas constant and T is the reaction temperature.

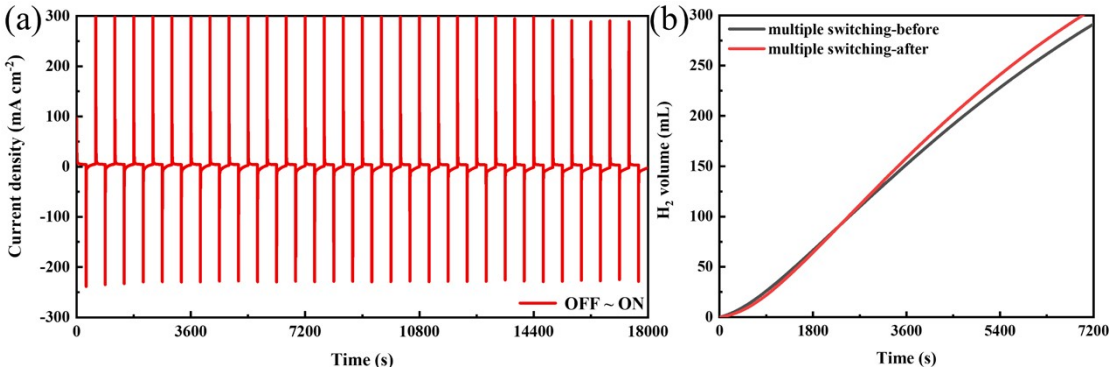


**Fig. S9** (a) The multi-cycle switching curve and (b) the curves of hydrogen volumes before and after the multi-cycle switching test in 1 M NaOH with 0.05 M $NaBH_4$.

A 30-cycle ON/OFF switching test was carried out to explore the stability of NiMoN@NC catalyst (Fig. S9a, ESI†). It can be seen that the $H_2$ volume lines and the HGRs (Fig. S9b, ESI†) before and after the multi-cycle test are very close to each other, indicating the outstanding reproducibility and remarkable stability of NiMoN@NC.

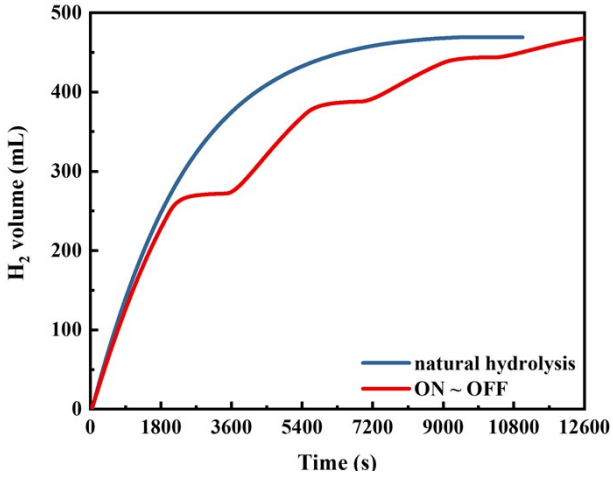


**Fig. S10** The curves of hydrogen volume vs time derived from the continuous $BH_4^-$ hydrolysis and the ON/OFF switching hydrolysis, the area of NiMoN@NC catalysts is 1 × 2 cm$^2$.

The influence of the ON/OFF switching on the hydrogen production efficiency was explored by comparing the total hydrogen volume generated in continuous hydrolysis with that in ON/OFF switching as shown in Fig. S10 (ESI†). The $H_2$ volumes generated in continuous ON and ON/OFF tests are 469.0 mL and 467.6 mL respectively, which both are approximately close to the theoretical value of 470.4 ml.

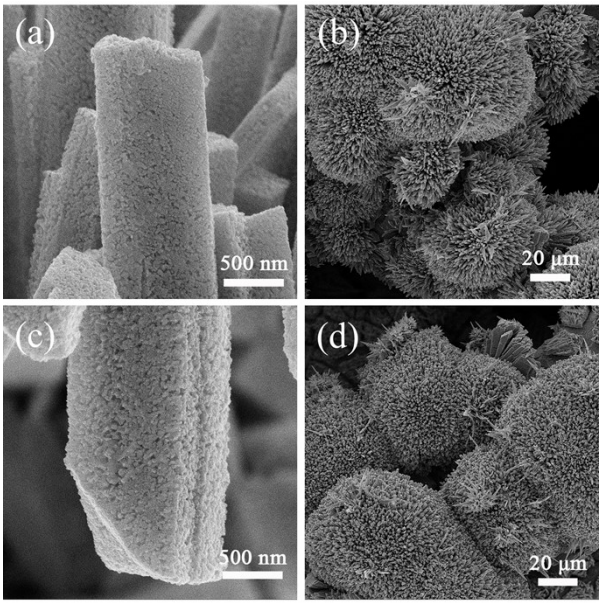


**Fig. S11** SEM images of NiMoN@NC after (a, b) ON and (c, d) OFF treatments.

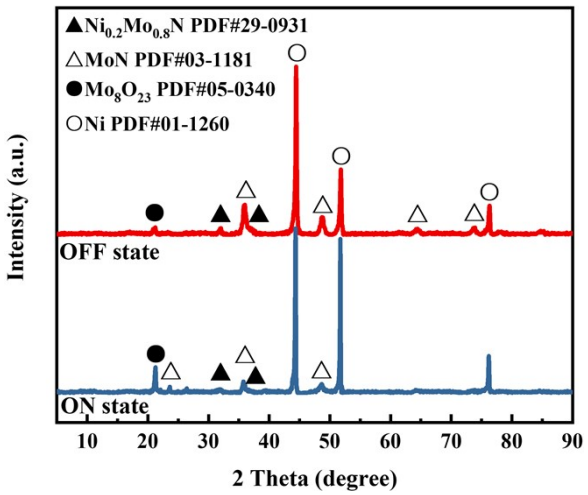


**Fig. S12** XRD patterns of NiMoN@NC after ON and OFF treatments.

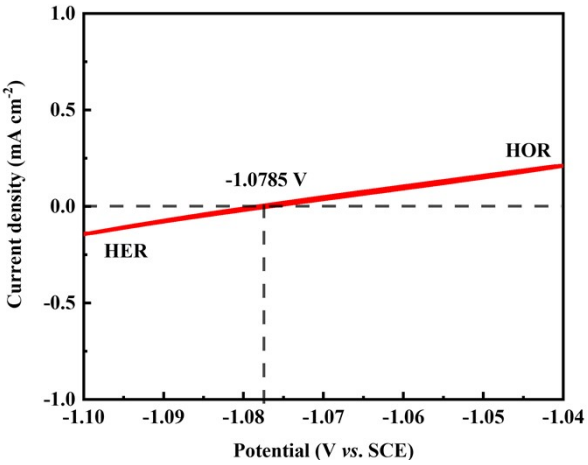


**Fig. S13** CV curves of hydrogen electrode reactions on the Pt wire with respect to SCE in 1 M NaOH with 0.05 M $NaBH_4$.

**Table S1** The comparison of the HGR and $E_a$ of different catalysts in recent reports.

| Catalyst | Reaction solution | Temperature (K) | HGR (mL $g^{-1}$ $min^{-1}$) | $E_a$ (kJ $mol^{-1}$) | Ref. |
|---|---|---|---|---|---|
| **NiMoN@NC** | **1 M NaOH + 0.05 M $NaBH_4$** | **298** | **74.3** | **33.16** | **This work** |
| ZnCo/Ti | 1 M NaOH + 0.05 M $NaBH_4$ | 298 | ＜39 | 42.00 | 2 |
| $Cu_{85}Co_{15}$ | 0.25 M NaOH + 0.25 M $NaBH_4$ | 353 | 3300 | 13.90 | 3 |
| $Co_3O_4$ NA/Ti | 1 wt.% NaOH + 1wt.% $NaBH_4$ | 298 | 1940 | 59.84 | 4 |
| Co@NMGC | 1 wt.% NaOH + 1.5 wt.% $NaBH_4$ | 298 | 3575 | 35.20 | 5 |
| CoP NA/Ti | 1 wt.% NaOH + 1wt.% $NaBH_4$ | 293 | 6500 | 40.90 | 6 |
| NiCoP NA/Ti | 1 wt.% NaOH + 0.5 wt.% $NaBH_4$ | 303 | 3016.79 | 52.68 | 1 |
| $Ni_2P$ NA/NF | 1wt.% AB | 298 | 42.3 ($mol_{H2}$ $mol_{Ni2P}^{-1}$ $min^{-1}$) | 44.00 | 7 |
| Ni-nanogel | 0.095 g $NaBH_4$ in 50 g water | 318 | - | 47.82 | 8 |
| $FeCo_2O_4$ | 5 wt.% NaOH + 1wt.% $NaBH_4$ | 298 | 2251 | 44.98 | 9 |
| Ru-Fe/GO | 1 wt.% NaOH + 10 wt.% $NaBH_4$ | 298 | 473 | 59.33 | 10 |
| CNSs@Co | 0.25 M NaOH + 0.25 M $NaBH_4$ | 303 | 7447 | 40.79 | 11 |
| CHNA/Ti | 1 wt.% NaOH + 1wt.% $NaBH_4$ | 298 | ~4000 | 39.78 | 12 |

**Table S2** The relative contents of N and O species obtained from XPS spectra analysis of NiMoN@NC-ON and NiMoN@NC-OFF.

| Species | NiMoN@NC-ON | NiMoN@NC-OFF |
|---|---|---|
| M-N | 39.3% | 31.6% |
| Pyridinic-N | 30.7% | 31.2% |
| Pyrrolic-N | 26.5% | 32.4% |
| Graphitic-N | 3.5% | 4.8% |
| Mo-O | 29.5% | 43.4% |
| C-O | 5.4% | 6.8% |

## References


1. K. Li, M. Ma, L. Xie, Y. Yao, R. Kong, G. Du, A. M. Asiri and X. Sun, *Int. J. Hydrogen Energy*, 2017, **42**, 19028-19034.
2. L. Tamašauskaitė-Tamašiūnaitė, S. Lichušina, A. Balčiūnaitė, A. Zabielaitė, D. Šimkūnaitė, J. Vaičiūnienė, A. Selskis and E. Norkus, *ECS Trans.*, 2014, **61**, 49-58.
3. S. Eugénio, U. B. Demirci, T. M. Silva, M. J. Carmezim and M. F. Montemor, *Int. J. Hydrogen Energy*, 2016, **41**, 8438-8448.
4. Y. Huang, K. Wang, L. Cui, W. Zhu, A. M. Asiri and X. Sun, *Catal. Commun.*, 2016, **87**, 94-97.
5. J. Li, X. Hong, Y. Wang, Y. Luo, P. Huang, B. Li, K. Zhang, Y. Zou, L. Sun, F. Xu, F. Rosei, S. P. Verevkin and A. A. Pimerzin, *Energy Storage Mater.*, 2020, **27**, 187-197.
6. L. Cui, Y. Xu, L. Niu, W. Yang and J. Liu, *Nano Res.*, 2016, **10**, 595-604.
7. C. Tang, L. Xie, K. Wang, G. Du, A. M. Asiri, Y. Luo and X. Sun, *J. Mater. Chem. A*, 2016, **4**, 12407-12410.
8. H. Cai, L. Liu, Q. Chen, P. Lu and J. Dong, *Energy*, 2016, **99**, 129-135.
9. S. Hao, L. Yang, L. Cui, W. Lu, Y. Yang, X. Sun and A. M. Asiri, *Nanotechnology*, 2016, **27**, 46LT03.
10. Y. Zhang, J. Zou, Y. Luo and F. Wang, *Fuller. Nanotub. Carbon Nanostruct.*, 2020, **28**, 786-793.
11. H. Zhang, G. Xu, L. Zhang, W. Wang, W. Miao, K. Chen, L. Cheng, Y. Li and S. Han, *Renew. Energy*, 2020, **162**, 345-354.
12. L. Cui, X. Sun, Y. Xu, W. Yang and J. Liu, *Chemistry*, 2016, **22**, 14831-14835.